Molecular Weight Distribution in Emulsion Polymerization: Role of Active Chain Compartmentalization

Alessandro Ghielmi, Giuseppe Storti, and Massimo Morbidelli*

Laboratorium für Technische Chemie, CAB, ETH Zürich, Universitätstrasse 6, CH-8092 Zürich, Switzerland

W. Harmon Ray

Department of Chemical Engineering, University of Wisconsin, Madison, Wisconsin 53706

Received April 23, 1998; Revised Manuscript Received July 27, 1998

ABSTRACT: A comparison of the results of two models with different levels of complexity has shown that errors can be made in the calculation of the polydispersity ratio of a polymer, produced in emulsion in the presence of termination by combination, if compartmentalization is not taken into account by properly considering the distribution of the lengths of the pairs of chains belonging to the same particle. These errors have been shown to be significant for values of the average number of free radicals per particle between about 0.4 and 2, which are typical of many emulsion systems. Accounting correctly for compartmentalization becomes crucial when the termination by combination mechanism is responsible for gelation, as in the case where branching through chain transfer to polymer is present in the system. The nature of the effects of compartmentalization on molecular weight has been analyzed both from a physical and a mathematical point of view. The importance of using a detailed model has been discussed for three polymerization systems: styrene, methyl methacrylate, and vinyl acetate.

1. Introduction

Besides affecting the kinetics of a free-radical polymerization with respect to homogeneous and suspension processes, emulsion systems have a great influence on the molecular weight of the final polymer. Since the active chains grow segregated (or *compartmentalized*) in the polymer particles and cannot terminate with chains growing in different polymer particles, faster reaction rates and larger molecular weights are achieved. To account for both these aspects, models specific to the emulsion process have been developed in the literature.

With a focus on molecular weight modeling, the first efforts are to be attributed to Katz, Shinnar and Saidel, who developed a model[1] consisting of coupled partial differential equations whose solution permits the desired molecular weight distribution (MWD) to be obtained. This however requires extensive numerical computation. Moreover, Katz et al. did not take into account some important reaction mechanisms, such as chain-transfer reactions and termination by disproportionation.

In the framework of a most general model for the emulsion polymerization process, Min and Ray derived through a kinetic approach partial differential equations for the evaluation of the molecular weight distribution of both the active and the dead polymer chains.[2] These equations accounted for all of the most typical mechanisms of chain termination, i.e., chain transfer to monomer or chain-transfer agent (CTA) and bimolecular termination by combination and by disproportionation.

In a successive work, Lichti et al.[3] showed that the knowledge of the MWD of the active chains is insufficient for the calculation of the distribution of the terminated polymer in the presence of termination by combination, since this reaction mechanism only couples the lengths of those pairs of chains belonging to the same particles, and not of any pair of chains in the system. The chain length distribution (CLD) of the *pairs* of chains belonging to the same particles is therefore required. To this aim, the concept of "doubly distinguished particles" was introduced. A particular case (zero-one-two system controlled by termination by combination) was examined in detail[4] to show that the instantaneous polydispersity would be incorrectly calculated by ignoring this specific requirement of compartmentalization.

More recently several kinetic models for the calculation of the MWD of *branched* polymers produced in emulsion have been published.[5−8] None of these account for the length distribution of pairs of chains belonging to the same particles, as required by Lichti and coworkers, and therefore estimate incorrectly the effect of compartmentalization on molecular weight in the presence of termination by combination.

To fill this lack, Ghielmi et al. proposed a kinetic model based on the concept of doubly distinguished particles for the evaluation of the MWD of long-chain branched[9] and cross-linked[10] polymers produced in emulsion. This model is an extension of the model proposed by Lichti et al. for linear chains.

A method for the MWD calculation of branched polymers produced in emulsion had been previously proposed by Tobita et al.[11] This method, based on the Monte Carlo technique, permits the treatment of complex effects such as chain compartmentalization and chain length dependent reaction rates. However, it suffers from the disadvantages typical of Monte Carlo methods, which are time consuming and provide no insight in the studied process, thus being seldom used in practice.

The aim of the present work is to perform an extensive analysis of the role of compartmentalization in determining the MWD characteristics in the presence

* To whom correspondence should be addressed.

10.1021/ma980657t CCC: $15.00
Published on Web 09/24/1998

of termination by combination, both for linear and for branched polymers. Significant information can be gained by analyzing the differences between a model ("detailed model") accounting for the CLD of the pairs of active chains belonging to the same particle, such as the model by Ghielmi et al., and another model ("simplified model") which limits itself to the calculation of the CLD of the active chains, such as that proposed by Min and Ray. Such an analysis has been carried out both in terms of instantaneous properties, which can be directly related to the reaction mechanisms active in the system, and of cumulative properties, which are those of interest in applications.

2. Model Summary

The derivation of the detailed model's equations, accounting for the length distribution of the pairs of chains belonging to the same particle (doubly distinguished particle distribution) can be found elsewhere.[9,10] Here we present in concise form the final equations (section 2.1), focusing mainly on the meaning of the calculated distributions and on the level of detail which they permit.

To compare the model predictions to those of a model neglecting the effect of compartmentalization on the length of the chains terminated by combination, a simplified version of the model is presented in section 2.2. The equations are presented in analogy to those of the detailed model to make the comparison between the two models straightforward. However, despite the different form, they are conceptually equivalent to those developed by Min and Ray.[2]

2.1. Detailed Model. The chain length distribution of the active polymer is represented, in the approach developed by Lichti et al.,[3] by the distribution of the singly distinguished particles, $N_i'(t,t')$. This quantity represents the fraction of particles containing i active chains, one of which (the distinguishing chain) was born at time t and is still growing at time $t + t'$. The length of the distinguishing chain is given by $n = \alpha t'$, where $\alpha = k_p C_m$ is the frequency of addition of monomer units.

When dealing with branched polymers,[9,10] a new distribution with an additional internal coordinate has to be defined: $B_i'(t,t',n')$. This represents the fraction of particles containing i active chains, one of which, branched, was born or reborn (through chain transfer to polymer) at time t and is still active at time $t + t'$. Parameter n' represents the *prelife* of the chain, i.e., the number of monomer units added by the distinguishing chain during all its previous growth periods or incorporated by cross-linking during the current one, or, equivalently, the number of monomer units belonging to the chain which have not been added by propagation to monomer in the last growth period. At time $t + t'$, the length of the chain is thus given by $n = n' + \alpha t'$.

Note that the knowledge of distributions $N_i'(t,t')$ and $B_i'(t,t',n')$ is completely equivalent to the knowledge of the CLD of the active polymer, since the length of the distinguishing chain is identified by the internal coordinates n' and t'.

With reference to the kinetic scheme summarized in Table 1, accounting for both chain transfer to polymer and cross-linking as sources of branching, the population balance equations governing the two singly distinguished particle distributions are reported here below together with the relevant initial conditions. For the sake of brevity, the matrix form of the equations has been selected:[9,10]

$$\frac{\partial \underline{\mathbf{N}}'(t, t')}{\partial t'} = \underline{\underline{\mathbf{A}}}(t)\underline{\mathbf{N}}'(t, t') \tag{1}$$

$$\frac{\partial \underline{\mathbf{B}}'(t, t', n')}{\partial t'} = \underline{\underline{\mathbf{A}}}(t)\underline{\mathbf{B}}'(t, t', n') + \int_0^{n'} k_p^* \gamma \underline{\mathbf{B}}'(t, t', n' - m) m D(t, m)\, \mathrm{d}m + k_p^* \gamma \underline{\mathbf{N}}'(t, t') n' D(t, n') \tag{2}$$

$$N_i'(t, t' = 0) = \rho N_{i-1}(t) + f i N_i(t) \tag{3}$$

$$B_i'(t, t' = 0, n') = k_{fp} i N_i(t) n' D(t, n') \tag{4}$$

All symbols are defined in the Glossary. Quantities $\underline{\mathbf{N}}'(t,t')$ and $\underline{\mathbf{B}}'(t,t',n')$ are the column vectors for the $N_i'(t,t')$ and $B_i'(t,t',n')$ distributions, respectively. In the initial conditions, $N_i(t)$ represents the fraction of particles containing i radicals at time t and is calculated from the Smith−Ewart equations.[12] Parameter $f = k_{fm}C_m + k_{ft}C_t - k$ is the pseudo-first-order rate coefficient for the transfer events (to monomer and to CTA) which do not result in short radical desorption from the particles.[4] Note that by introducing this parameter, a correction is made to the equations presented in refs 9 and 10, which assume that active chains of any length can desorb, ceasing their activity. Here instead, the classical assumption[13−15] is made that the desorbing species are only the short radicals produced by chain transfer to a small molecule, which is physically more reasonable. Accordingly, the introduction of parameter f removes the assumption which prevented the correct application of the equations in refs 9 and 10 to systems affected by strong radical desorption.

In eqs 1−4, the difference between the two cases of linear and branched distinguishing chain lies in the terms accounting for the crosslinking reaction and in the initial conditions. As far as crosslinking is concerned, the difference arises because this mechanism can give origin to branched chains but not to linear ones. In the corresponding generation terms, parameter γ indicates the fraction of unsaturated monomer units (i.e., those that can give crosslinking) in the dead chain. This fraction is assumed to be independent of chain length, but to vary on an average with conversion. With respect to the initial conditions, a new linear active chain is formed by radical entry from the water phase or by chain transfer to a small molecule (with the exception of those transfer events resulting in desorption), while chain transfer to a dead polymer chain of length n', belonging to the distribution represented by $D(t, n')$, produces a new branched active chain with prelife n'.

Finally, $\underline{\underline{\mathbf{A}}}(t)$ is a band matrix of coefficients $a_{i,j}$ with zero value, except for the following:

$$a_{i,i-1} = \rho \quad a_{i,i+1} = ik \quad a_{i,i+2} = i(i+1)c$$

$$a_{i,i} = -[\rho + ik + i(i-1)c + f + (k_{fp} + k_p^*\gamma)\sigma^{(1)}]$$

where $\sigma^{(1)}$ is the first-order moment of the dead polymer length distribution. It should be observed that minor modifications arise for $i = 1$, $N - 1$, and N, where N indicates the maximum number of active chains per particle.

As discussed above, when bimolecular terminations by combination are considered an additional problem

arises, i.e., the two colliding chains have to be *in the same particle* and both their lengths must be specified. This is a requirement of compartmentalization and, to be properly accounted for, a new distribution of *pairs* of distinguished active chains has to be defined. In the case of a pair of linear chains, the distribution $N_i''(t,t',t'')$ is introduced, where t and $t + t'$ identify the birth times of the first (older) and the second (younger) chain in the pair, being $t' + t''$ and t'' the corresponding lifetimes at time $t + t' + t''$. When branched chains are considered, other three different distributions have to be defined: $O_i''(t,t',t'',n')$, $Y_i''(t,t',t'',n'')$, and $B_i''(t,t',t'',n',n'')$, depending upon which chain of the pair is branched (the older, the younger, or both). In this case, n' and n'' characterize the prelives of the older and of the younger chain, respectively, the length of which is given by $n' + \alpha(t' + t'')$ and $n'' + \alpha t''$.

The population balance equations for the distributions of the doubly distinguished particles are reported here below, once again in matrix form; $\mathbf{N}_i''(t,t',t'')$, $\mathbf{O}_i''(t,t',t'',n')$, $\mathbf{Y}_i''(t,t',t'',n'')$, and $\mathbf{B}_i''(t,t',t'',n',n'')$ are the column vectors corresponding to the four doubly distinguished distributions:

$$\frac{\partial \underline{\mathbf{N}}'(t, t', t'')}{\partial t''} = \underline{\underline{\mathbf{D}}}(t)\underline{\mathbf{N}}''(t, t', t'') \tag{5}$$

$$\frac{\partial \underline{\mathbf{O}}''(t, t', t'', n')}{\partial t''} = \underline{\underline{\mathbf{D}}}(t)\underline{\mathbf{O}}''(t, t', t'', n') + \int_0^{n'} k_p^*\gamma \underline{\mathbf{O}}''(t, t', t'', n' - m)mD(t, m)\,\mathrm{d}m + k_p^*\gamma \underline{\mathbf{N}}''(t, t', t'')n'D(t, n') \tag{6}$$

$$\frac{\partial \underline{\mathbf{Y}}''(t, t', t'', n')}{\partial t''} = \underline{\underline{\mathbf{D}}}(t)\underline{\mathbf{Y}}''(t, t', t'', n'') + \int_0^{n''} k_p^*\gamma \underline{\mathbf{Y}}''(t, t', t'', n'' - m)mD(t, m)\,\mathrm{d}m + k_p^*\gamma \underline{\mathbf{N}}''(t, t', t'')n''D(t, n'') \tag{7}$$

$$\frac{\partial \underline{\mathbf{B}}''(t, t', t'', n', n'')}{\partial t''} = \underline{\underline{\mathbf{D}}}(t)\underline{\mathbf{B}}''(t, t', t'', n'') + \int_0^{n'} k_p^*\gamma \underline{\mathbf{B}}''(t, t', t'', n' - m, n'')mD(t, m)\,\mathrm{d}m + \int_0^{n''} k_p^*\gamma \underline{\mathbf{B}}''(t, t', t'', n', n'' - m)mD(t, m)\,\mathrm{d}m + k_p^*\gamma \underline{\mathbf{Y}}''(t, t', t'', n'')n'D(t, n') + k_p^*\gamma \underline{\mathbf{O}}''(t, t', t'', n')n''D(t, n'') \tag{8}$$

$$N_i''(t, t', t'' = 0) = \rho N_{i-1}'(t, t') + f(i - 1)N_i'(t, t') \tag{9}$$

$$O_i''(t, t', t'' = 0, n') = \rho B_{i-1}'(t, t', n') + f(i - 1)B_i'(t, t', n') \tag{10}$$

$$Y_i''(t, t', t'' = 0, n'') = k_{fp}(i - 1)\, N_i'(t, t')n''D(t, n'') \tag{11}$$

$$B_i''(t, t', t'' = 0, n', n'') = k_{fp}(i - 1)\, B_i'(t, t', n')n''D(t, n'') \tag{12}$$

The coefficients $d_{i,j}$ of the band matrix $\underline{\underline{\mathbf{D}}}(t)$ have zero value, except for the following:

$$d_{i,i-1} = \rho \quad d_{i,i+1} = (i - 1)k \quad d_{i,i+2} = i(i - 1)c$$

$$d_{i,i} = -[\rho + ik + i(i - 1)c + 2f + 2(k_{fp} + k_p^*\gamma)\sigma^{(1)}]$$

Minor modifications are required for $i = 2$, $N - 1$, and N.

Table 1. Kinetic Scheme

kinetic event	frequency
radical entry in the particles	
$R_w^\bullet \xrightarrow{k_e} R_0^\bullet$	ρ
propagation	
$R_n^\bullet + M \xrightarrow{k_p} R_{n+1}^\bullet$	$k_pC_m = \alpha$
chain transfer to monomer	
$R_n^\bullet + M \xrightarrow{k_{fm}} P_n + R_0^\bullet$	$k_{fm}C_m$
chain transfer to CTA	
$R_n^\bullet + T \xrightarrow{k_{ft}} P_n + R_0^\bullet$	$k_{ft}C_t$
desorption	
$R_0^\bullet \xrightarrow{k_d} R_w^\bullet$	k_d
bimolecular termination by combination	
$R_n^\bullet + R_m^\bullet \xrightarrow{k_{tc}} P_{n+m}$	$\frac{k_{tc}}{2N_Av_P} = c_c$
bimolecular termination by disproportionation	
$R_n^\bullet + R_m^\bullet \xrightarrow{k_{td}} P_n + P_m$	$\frac{k_{td}}{2N_Av_P} = c_d$
chain transfer to polymer	
$R_n^\bullet + P_m \xrightarrow{k_{fp}} P_n + R_m^\bullet$	$k_{fp}m[P_m]$
cross-linking	
$R_n^\bullet + P_m \xrightarrow{k_p^*} R_{n+m}^\bullet$	$k_p^*m\gamma[P_m]$

In order to evaluate the CLD of the terminated polymer, which is that of interest, it is convenient to subdivide the dead polymer into two parts, the first one collecting all the chains terminated by any mechanism but bimolecular combination and the second one those produced by this last termination mechanism only.

Focusing on the first portion of dead polymer, two distributions may be conveniently defined: $S^M(t_e, t')$ and $G^M(t_e, t', n')$. These are the cumulative distributions at reaction time t_e of the dead macromolecules with length $n = \alpha t'$ and $n = n' + \alpha t'$ in the case of linear and branched chains, respectively.

The corresponding material balances for a batch reactor are given by

$$\frac{\mathrm{d}[v_P S^M(t_e, t')]}{\mathrm{d}t_e} = \left\{(f + k + k_{fp}\sigma^{(1)})\sum_{i=1}^{N} N_i'(t_e - t', t') + \frac{\rho}{N}N_N'(t_e - t', t') + 2c_d\sum_{i=2}^{N}(i - 1)N_i'(t_e - t', t') - (k_{fp} + k_p^*\gamma)(at')S^M(t_e, t')\bar{n}\right\}\frac{1}{N_A} \tag{13}$$

$$\frac{\mathrm{d}[v_P G^M(t_e, t', n')]}{\mathrm{d}t_e} = \left\{(f + k + k_{fp}\sigma^{(1)})\sum_{i=1}^{N} B_i'(t_e, - t', t', n') + \frac{\rho}{N}B_N'(t_e - t', t', n') + 2c_d\sum_{i=2}^{N}(i - 1)B_i'(t_e - t', t', n') - (k_{fp} + k_p^*\gamma)(n' + at')G^M(t_e, t', n')\bar{n}\right\}\frac{1}{N_A} \tag{14}$$

where v_P is the volume of a polymer particle. Note that the singly distinguished particle distributions only are required to solve the previous differential equations. All termination mechanisms (apart from combination) are accounted for: chain transfer to small molecule and to polymer, entry in state N particles (i.e., particles containing N radicals), and disproportionation; moreover, some consumption terms due to chain transfer to polymer and to cross-linking are also present.

In the case of bimolecular termination by combination, four different cumulative chain length distributions are defined (S^C, V^C, W^C, and G^C), depending upon the chain type (linear or branched) and birth time of the colliding pair. To their evaluation, the knowledge of the doubly distinguished particle distributions is essential and the following material balances are required:

$$\frac{\mathrm{d}[v_P S^C(t_e, t', t'')]}{\mathrm{d}t_e} = \{2c_c\sum_{i=2}^{N} N_i''(t_e - t' - t'', t', t'') - (k_{fp} + k_p^*\gamma)(\alpha t' + 2\alpha t'')S^C(t_e, t', t'')\bar{n}\}\frac{1}{N_A} \quad (15)$$

$$\frac{\mathrm{d}[v_P V^C(t_e, t', t'', n')]}{\mathrm{d}t_e} = \{2c_c\sum_{i=2}^{N} O_i''(t_e - t' - t'', t', t'', n') - (k_{fp} + k_p^*\gamma)(n' + \alpha t' + 2\alpha t'')V^C(t_e, t', t'', n')\bar{n}\}\frac{1}{N_A} \quad (16)$$

$$\frac{\mathrm{d}[v_P W^C(t_e, t', t'', n'')]}{\mathrm{d}t_e} = \{2c_c\sum_{i=2}^{N} Y_i''(t_e - t' - t'', t', t'', n'') - (k_{fp} + k_p^*\gamma)(n'' + \alpha t' + 2\alpha t'')W^C(t_e, t', t'', n'')\bar{n}\}\frac{1}{N_A} \quad (17)$$

$$\frac{\mathrm{d}[v_P G^C(t_e, t', t'', n', n'')]}{\mathrm{d}t_e} = \{2c_c\sum_{i=2}^{N} B_i''(t_e - t' - t'', t', t'', n', n'') - (k_{fp} + k_p^*\gamma)(n' + n'' + \alpha t' + 2\alpha t'')G^C(t_e, t', t'', n', n'')\bar{n}\}\frac{1}{N_A} \quad (18)$$

Note that these equations are very similar, the only difference appearing in the terms of consumption due to chain transfer to polymer and cross-linking, where the overall length of the dead chain originated from the combination is different.

The system of differential equations for both the active (eqs 1, 2, and 5−8) and the dead (eqs 13, 14, and 15−18) polymer may be effectively solved by the method of moments; accordingly, integration upon all possible values of current lifetime and prelife is performed, yielding a set of linear algebraic equations for the moments of the active chains and a system of ordinary differential equations to be integrated in the experimental time t_e for the moments of the dead polymer.

Table 2. Numerical Values of the Model Parameters Used for the Calculations of Instantaneous Properties[a]

parameter	value
C_m	5.7×10^{-3} mol cm^{-3}
k	1.3×10^{-3} s^{-1}
k_{fm}	10 cm^3 (mol s)$^{-1}$
k_{fp}	10 cm^3 (mol s)$^{-1}$
k_p	2.6×10^5 cm^3 (mol s)$^{-1}$
k_p^*	5 cm^3 (mol s)$^{-1}$
k_{tc}	1.16×10^9 cm^3 × (mol s)$^{-1}$
k_{td}	0 cm^3 (mol s)$^{-1}$
v_P	1.21×10^{-15} cm^3
$\sigma^{(0)}$	2.38×10^{-7} mol cm^{-3}
$\sigma^{(1)}$	3.22×10^{-3} mol cm^{-3}
$\sigma^{(2)}$	105.3 mol cm^{-3}

[a] The moments of $\sigma^{(k)}$ of the dead polymer are referred to the particle phase volume.

In the case of branched polymers, the difficulties arising in the description of very broad CLDs and of gel formation have been overcome by applying the "numerical fractionation" technique for the solution of the equations.[16,9]

2.2. Simplified Model. In this section, a modified version of the previous model, which we shall refer to as "simplified model" is presented. This is derived by following the same procedure developed by Min and Ray,[2] but using the formalism adopted in the detailed model above.

The main idea of this approach is to evaluate the rate of production of chains of length n due to the combination reaction in particles with i radicals by multiplying the rate of combination of chains of length l in particles of the same type by the probability that the coupling chain has a length $n - l$, and summing over all l values from 0 to n. The key assumption is that this probability is independent of the fact that a chain with the length of the first chosen chain is already present in the particle and can be consequently evaluated from the CLD of the active polymer in state i particles, without introducing a CLD for the pairs of chains. As discussed also in ref 2, this assumption is certainly valid if each particle contains a statistical number of growing chains; for a smaller number of growing chains per particle (say less than 10), this validity is less obvious. It is actually the validity of this assumption that we are discussing here.

In the approach which exploits the concepts of distinguished particles, this assumption leads to the significant simplification of ignoring the distribution of the doubly distinguished particles. In the case of linear chains, the rate of combination in state i particles of two radicals, one of current lifetime t' and the other of current lifetime t'', is given by the rate of combination of radicals with lifetime t', $2c_c(i-1)N_i'(t, t')$, times the probability that the coupling chain has a lifetime t'', $N_i'(t, t'')/iN_i$ (where this probability is assumed independent of t'). In the case of branched chains, it is enough to introduce the prelives of one or both chains.

Accordingly, with respect to the detailed model, the equations for calculating the doubly distinguished particle distributions (eqs 5−8) are omitted and eqs 15−18 are substituted by the following:

$$\frac{d[v_P \bar{S}^C(t_e, t', t'')]}{dt_e} = \left\{ 2c_c \sum_{i=2}^{N} (i-1) N_i'(t_e - t', t') \frac{N_i'(t_e - t'', t'')}{iN_i} - (k_{fp} + k_p^* \gamma)(\alpha t' + \alpha t'') \bar{S}^C(t_e, t', t'') \bar{n} \right\} \frac{1}{N_A} \quad (19)$$

$$\frac{d[v_P \bar{V}^C(t_e, t', t'', n')]}{dt_e} = \left\{ 2c_c \sum_{i=2}^{N} (i-1) B_i'(t_e - t', t', n') \frac{N_i'(t_e - t'', t'')}{iN_i} - (k_{fp} + k_p^* \gamma)(n' + \alpha t' + \alpha t'') \bar{V}^C(t_e, t', t'', n') \bar{n} \right\} \frac{1}{N_A} \quad (20)$$

$$\frac{d[v_P \bar{G}^C(t_e, t', t'', n', n'')]}{dt_e} = \left\{ 2c_c \sum_{i=2}^{N} (i-1) B_i'(t_e - t', t', n') \frac{B_i'(t_e - t'', t'', n'')}{iN_i} - (k_{fp} + k_p^* \gamma)(n' + n'' + \alpha t' + \alpha t'') \bar{G}^C(t_e, t', t'', n', n'') \bar{n} \right\} \frac{1}{N_A} \quad (21)$$

Here, distributions $\bar{S}^C(t_e, t', t'')$, $\bar{V}^C(t_e, t', t'', n')$, and $\bar{G}^C(t_e, t', t'', n', n'')$ are the distributions at time t_e of the dead polymer formed by combination at any reaction time from active chains of given current lifetimes t' and t'' and, in the case, prelives n' and n''.

The length of the resulting chain is given by $n = n' + n'' + \alpha(t' + t'')$ (with n' or n'' equal to zero, if the corresponding chain is linear).

Note that, different from the case of the detailed model, only three distributions are required: $\bar{S}^C(t_e, t', t'')$, $\bar{V}^C(t_e, t', t'', n')$, and $\bar{G}^C(t_e, t', t'', n', n'')$. More specifically, distributions $V^C(t_e, t', t'', n')$ and $W^C(t_e, t', t'', n'')$ of the detailed model are replaced by a single distribution $\bar{V}^C(t_e, t', t'', n')$. This happens because the simplified model does not take into account which of the two chains of the pair is first born (or reborn) and, accordingly, saying that one of the two chains is branched and the other linear is enough to distinguish them. This also reflects the reduced level of detail of the simplified model.

In conclusion, the simplified version of the model is constituted by eqs 1, 2, 13, 14, 19−21. From the mathematical point of view, the resulting system is closely similar to the one obtained in the case of the detailed model. Moreover, the numerical solving procedure is the same and requires an equivalent computational effort.

3. Illustrative Calculations

In the following a comparison between the MWD properties calculated by the two models is performed. In section 3.1, the analysis is performed in terms of instantaneous properties, i.e., those of the infinitesimal amount of dead polymer produced at a particular instant during the polymerization reaction. In this case, only the equations detailed in the previous section are required. Even though the meaning of these quantities becomes less clear when dealing with branching systems, we believe that the comparison remains significant and elucidates interesting features of the two approaches.

In section 3.2, an analogous comparison is carried out in terms of MWD properties of the polymer actually produced, i.e., in terms of cumulative molecular weights. In this case, the previous equations have to be coupled to a model able to account for the evolution during the emulsion polymerization of all those quantites which influence the MWD of the product, for instance particle size, monomer concentration in the particles and so on. In particular, the model proposed by Storti et al.[17] has been used; main assumptions are particle size monodispersion and thermodynamic equilibrium conditions for the phase partitioning of the monomer.

3.1. Instantaneous Properties. The numerical values of the model parameters used for the calculation of the instantaneous properties are summarized in Table 2. Each of these values applies when the corresponding reaction mechanism is considered to be operative; if not, it is set equal to zero.

In all cases the instantaneous polydispersity ratio, P_d^i, is shown as a function of the average number of active chains per particle, $\bar{n}$. The variation of $\bar{n}$ has been obtained by changing the value of the entry rate of the active radicals from the aqueous phase to the particles, ρ. Note that while low $\bar{n}$ values are typical of emulsion polymerization systems, at increasing values of the number of active chains per particle the behavior of each particle approaches that of a bulk system and any compartmentalization effect is expected to vanish.

In Figures 1 and 3 the case of linear chains is examined; thus, k_{fp} and k_p^* are set to zero.

In Figure 1 combination has been considered as the only operating termination mechanism, and both chain transfer to monomer and desorption have been neglected, i.e., $k = k_{fm} = 0$. By inspection of the calculated curves (continuous curve for the detailed model and broken curve for the simplified model) it appears that the same number-average degree of polymerization (Figure 1a) is predicted, since the two curves are in fact superimposed. However, the different behavior of the polydispersity ratio predicted by the two models (Figure 1b) proves the need for taking into account chain compartmentalization through the doubly distinguished particle distributions.

Note that the continuous curve exhibits two physically significant extreme values, i.e., $P_d^i = 2$ at $\bar{n} = 0.5$ and P_d^i approaching 1.5 at large $\bar{n}$ values. At large $\bar{n}$ values, $P_d^i = 1.5$ corresponds to the value for bulk polymerization with dominant bimolecular termination by combination. This result is physically sound since in this situation the particles can be regarded as minibulks. At $\bar{n} = 0.5$, instead, the situation is that of chains mainly growing undisturbed in state one particles to very great lengths (see Figure 1a). This is due to very low entry frequencies. When a new radical enters the particle, bimolecular termination by combination occurs rapidly ($c \gg \rho$), so that the units added to the two chains between the entry and the termination are negligible with respect to the final length of the chain. The termination mechanism can thus be compared to a monomolecular termination mechanism, because it preserves the length of the growing chain.

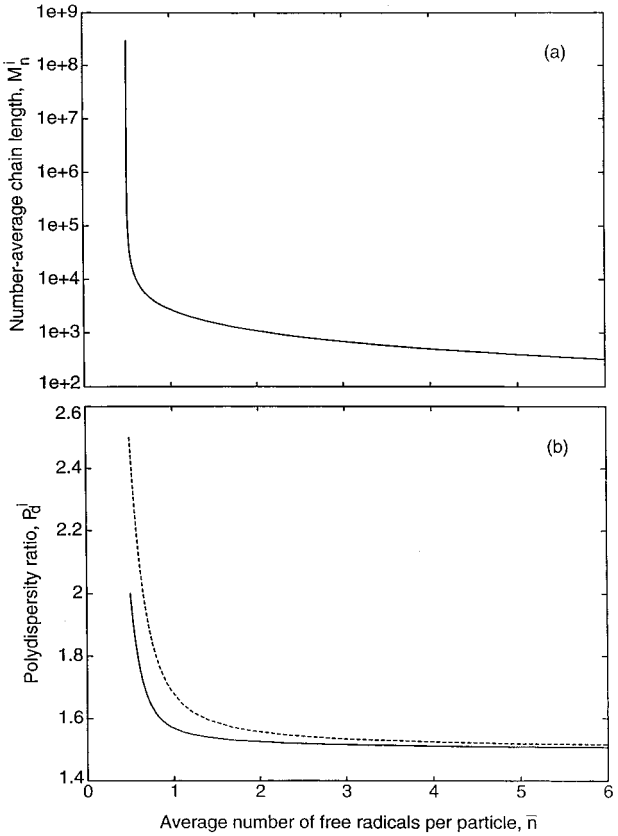

Figure 1. (a) Number-average chain length and (b) polydispersity ratio as a function of the average number of active chains per particle, $\bar{n}$. Parameter values as in Table 2 but with $k = k_{fm} = k_{fp} = k_p^* = 0$. Lines: (—) detailed model and (- - -) simplified model.

This does not necessarily mean that bimolecular termination is "instantaneous" upon entry, in the sense that it is faster than propagation, but just that the length of the chain is determined by the entry frequency rather than by that of combination. This termination mechanism corresponds to a polydispersity value of 2, which is indeed typical of monomolecular termination.

The situation examined here above at $\bar{n} = 0.5$ ($\rho \ll c$) also provides a good picture for understanding the need for the doubly distinguished particle description. Assuming that in these conditions the particles containing more than two radicals are negligible in number, the situation can be depicted as in Figure 2a. This figure shows a population of state one particles containing chains growing alone up to high lengths, corresponding to characteristic times τ_ρ given by the inverse of the entry frequency ρ. Upon entry of a second radical, a population of state two particles appears where the first chain is still growing but now a second chain grows along with it. The typical length of this second chain is determined by the bimolecular termination frequency c and corresponds to the characteristic time $\tau_c = 1/2c$. As $\rho \ll c$, $\tau_c \ll \tau_\rho$. Accordingly, two very different chain populations are present in the state two particles. The first chain population has a long characteristic lifetime τ_ρ, while the second has a short characteristic lifetime τ_c. This is illustrated in Figure 2b, where these two components of the N_2' distribution (distribution of the active chains in state two particles) are qualitatively shown. In all particles containing two chains, one chain belongs to the distribution with $\tau = \tau_\rho$ (broken curve in Figure 2b) and the other to the distribution with $\tau = \tau_c$

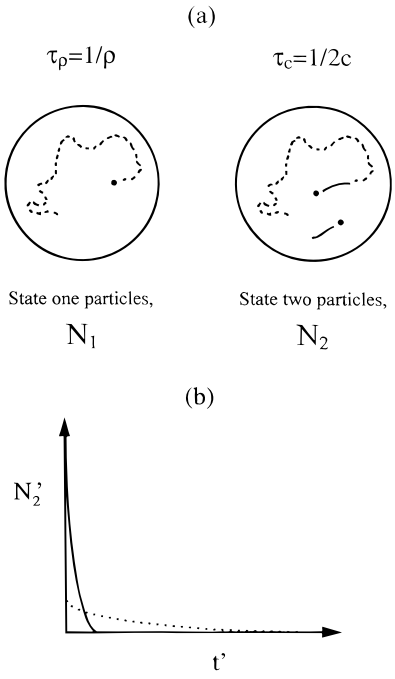

Figure 2. (a) Picture of the chain lengths in state one and two particles at entry frequencies much smaller than the bimolecular termination frequency. (b) Two components of the chain-length distribution in state two particles, with different characteristic lifetimes. Lines: (—) $\tau_c = 1/2c$ and (- - -) $\tau_\rho = 1/\rho$.

(solid curve in Figure 2b). It is clear that in a termination by combination event it can never happen that two chains belonging to the same of these distributions couple together. The doubly distinguished particle approach accounts for the presence of these two different chain populations through the idea of first-born and last-born chain. Given the distribution $N_2'(t, t', t'')$, the time t' during which the first-born chain grows alone is related to characteristic time τ_ρ, while the time t'' during which the two chains grow together is related to characteristic time τ_c. If this kind of description is not adopted, as in the simplified model, coupling of two chains belonging to the same component of distribution N_2' (solid or broken curve in Figure 2b) is allowed. Accordingly, a greater amount of short−short and long−long chain combination is admitted with respect to reality. This explains the larger polydispersity ratio calculated by the simplified model at $\bar{n} = 0.5$, as shown by the broken curve in Figure 1b. On the other hand, it has been shown in Figure 1a that the number-average chain length M_n^i is calculated correctly by the simplified model. This is due to the fact that it is just the way in which the active chains couple which is incorrectly described by this model, while the length of these chains and the number of the coupling events is computed correctly.

The physical considerations above can be confirmed analytically by writing the balance equations for the singly and doubly distinguished particles in the case where the polymer particles containing more than two active chains are negligible in number. The following balances for the singly distinguished particles result:

$$\frac{\partial N_1'(t, t')}{\partial t'} = -\rho N_1'(t, t') \tag{22}$$

$$\frac{\partial N_2'(t, t')}{\partial t'} = \rho N_1'(t, t') - (\rho + 2c) N_2'(t, t') \tag{23}$$

with initial conditions:

$$N'_1(t, t' = 0) = \rho N_0(t) \quad (24)$$

$$N'_2(t, t' = 0) = \rho N_1(t) \quad (25)$$

Remember that no desorption is assumed to take place ($k = 0$). Solution of system 22−23, accounting for the fact that $\rho \ll c$, yields

$$N'_1(t, t') = \rho N_0 e^{-\rho t'} \quad (26)$$

$$N'_2(t, t') = \frac{\rho^2 N_0}{2c} e^{-\rho t'} + \rho N_1 e^{-2ct'} \quad (27)$$

with $N_0 \simeq N_1 \simeq 0.5$. Observing the expression of N'_2, it can be seen that this is constituted by two exponential terms with different characteristic decay times, as depicted in Figure 2b. However, from expression 27 it is still not clear whether two chains belonging to the same particle can contribute to the same exponential term or not.

The rate of production at time t of terminated chains of a given length $\alpha\bar{t}$ is calculated by the simplified model as

$$\hat{S}^{C,s}(t, \bar{t}) = \frac{1}{2}\int_0^{\bar{t}} 2cN'_2(t, \bar{t} - t')\frac{N'_2(t, t')}{2N_2} dt' \quad (28)$$

This implies multiplication of distribution N'_2 by itself, with the appearence of terms arising from the multiplication of each exponential contribution $e^{-\rho t'}$ and $e^{-2ct'}$ by itself. These terms physically represent the short−short and long−long chain terminations which are in practice prevented by compartmentalization, and which cause an erroneous increase in the calculated polydispersity. Integral 28 can be carried out analytically, using eq 27 for $N'_2(t, t')$. This gives

$$\hat{S}^{C,s}(t,\bar{t}) = c^2\left\{\rho N_1 \bar{t} e^{-2c\bar{t}} + \frac{\rho^3 N_0}{4c^2}\bar{t} e^{-\rho\bar{t}} + \frac{\rho^2 N_0}{2c^2}[e^{-\rho\bar{t}} - e^{-2c\bar{t}}]\right\} \quad (29)$$

What is interesting in this expression is the appearence of the two terms of the form $\bar{t}e^{-a\bar{t}}$, typical of a bimolecular termination by combination mechanism. These terms are precisely those which arise from the combination of chains within each of the two distributions constituting the N'_2 distribution, the impossibility of which has been discussed above.

A correct analytical solution can be obtained by use of the doubly distinguished particle distribution. Assuming again a negligible amount of particles containing more than two radicals, the balance for $N''_2(t, t', t'')$ is given by

$$\frac{\partial N''_2(t, t', t'')}{\partial t''} = -(\rho + 2c)N''_2(t, t', t'') \quad (30)$$

with initial condition

$$N''_2(t, t', t'' = 0) = \rho N'_1(t, t') \quad (31)$$

This yields ($\rho \ll c$)

$$N''_2(t, t', t'') = \rho^2 N_0 e^{-\rho t'} e^{-2ct''} \quad (32)$$

In a different form, it appears again that the chains belonging to state two particles can be subdivided into two families, the first with characteristic lifetime $\tau_\rho = 1/\rho$ and the second with characteristic lifetime $\tau_c = 1/2c$. However, this time it appears that each one of the chains in a state two particle belongs to a distribution with a different characteristic lifetime.

The detailed model calculates the rate of formation at time t of terminated chains of length $\alpha\bar{t}$ as

$$\hat{S}^{C,d}(t, \bar{t}) = \int_0^{\bar{t}/2} 2cN''_2(t, \bar{t} - 2t'', t'') dt'' \quad (33)$$

By substitution of eq 32 in integral 33, it appears that only coupling of chains with different characteristic times is admitted. The analytical solution of integral 33 yields:

$$\hat{S}^{C,d}(t, \bar{t}) = \rho^2 N_0(e^{-\rho\bar{t}} - e^{-c\bar{t}}) \quad (34)$$

This time the terms of the form $\bar{t}e^{-a\bar{t}}$ do not appear. The bimolecular nature of the termination event under consideration appears from the fact that $\hat{S}^{C,d}(t, \bar{t} = 0) = 0$. However, at lifetimes $\bar{t} = \tau_c$, i.e., very short with respect to those achieved on an average, $\hat{S}^{C,d}(t, \bar{t}) \simeq \rho^2 N_0 e^{-\rho\bar{t}}$, i.e., the distribution has the form of that given by a monomolecular termination mechanism, implying $P_d^i = 2$.

The analysis above shows that situations exist where the lengths of the two colliding chains are correlated, so that the assumption of independence of the two lengths (see section 2.2) fails. In these cases, the simplified model is no longer valid. The nature of this correlation is analyzed in detail in section 4 from a statistical point of view.

At increasing $\bar{n}$ values, the broken curve in Figure 1b approaches the solid one. One expects this to happen at very high $\bar{n}$ values, in conditions where all particles can be considered as minibulks, i.e., they contain a statistical number of chains, which implies no correlation of the chain lengths. This is because all particles contain such a high number of chains that extracting a chain from a particle would cause no significant disturbance to the distribution of the chain lengths in that particle, which is the same as that in all the other particles. It follows that choosing a second chain to couple to the first from the same particle or from a different one is exactly the same. However, observing Figure 1b, it can be seen that the answers of the two models (detailed and simplified) are very close already at $\bar{n}$ values (e.g., $\bar{n} = 3$) which are much smaller than those required for all particles to be considered as minibulks. In these conditions, a large fraction of particles containing very few radicals (e.g., one or two) are still present. The analysis previously conducted at $\bar{n} = 0.5$, where the pairwise correlation between the chain lengths was explained on the basis of the fact that $\rho \ll c$, suggests that this correlation disappears when $\rho \gg c$, i.e., much before all particles contain a statistical number of active chains. In Figure 1b, we have in fact $\rho/c \to 0$ as $\bar{n} \to 0.5$, $\rho/c = 1$ at $\bar{n} = 0.9$ and $\rho/c = 16$ at $\bar{n} = 3$. This point will be better clarified in section 4 through statistical arguments.

A similar analysis can be made in the presence of both chain transfer to monomer and desorption, with the results shown in Figure 3. Due to the desorption mechanism, in this case the minimum value of $\bar{n}$ is zero. The value $P_d^i = 2$ calculated at $\bar{n} \to 0$, corresponds to

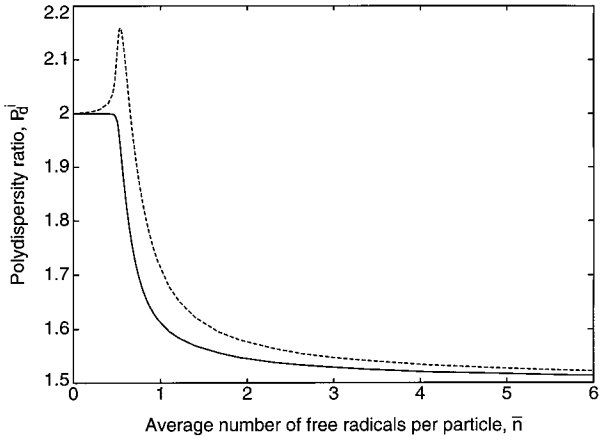

Figure 3. Polydispersity ratio as a function of the average number of active chains per particle, $\bar{n}$. Parameter values as in Table 2 but with $k_{fp} = k_p^* = 0$. Lines: (—) detailed model and (- - -) simplified model.

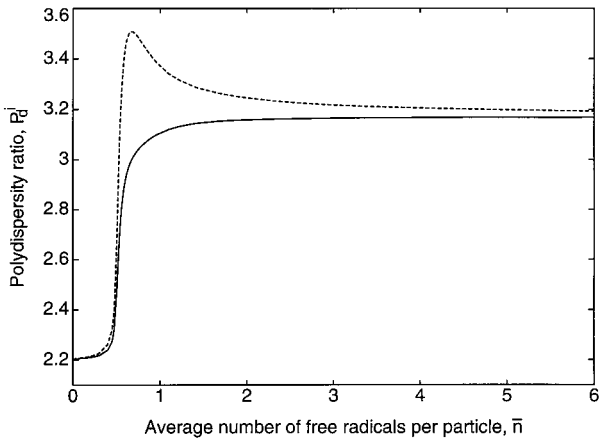

Figure 4. Polydispersity ratio as a function of the average number of active chains per particle, $\bar{n}$. Parameter values as in Table 2 but with $k_p^* = 0$. Lines: (—) detailed model and (- - -) simplified model.

dominant monomolecular termination. Both models predict this asymptotic value, since in these conditions particles in state two and consequently bimolecular terminations are completely negligible. However, differences arise around $\bar{n} = 0.5$, where the simplified model overestimates again the broadness of the MWD. Instead, the same M_n^i is predicted by the two models at all $\bar{n}$ values.

With reference to branched polymers, the case of chain transfer to polymer has first been considered. All the parameter values reported in Table 2 have been used, except for cross-linking which is considered to be absent ($k_p^* = 0$). Figure 4 shows that the two models predict significantly different polydispersity ratios. In particular, the simplified model calculates, as for the case of linear chains, larger P_d^i values than the detailed one, especially at $\bar{n}$ values between 0.5 and 1. The error introduced may be significant, more than 15% in the worst case. Again, the same M_n^i is predicted by the two models.

Similar results are obtained in the case of nonlinear chains produced by the cross-linking reaction (see Figure 5). For the calculations reported in this figure the numerical values of Table 2 have been used but $k_{fp} = 0$. In this case, the qualitative behavior of the polydispersity curves predicted by the two models is the same, exhibiting a maximum in both cases. However, significant discrepancies arise around $\bar{n}$ values typical of an emulsion polymerization system.

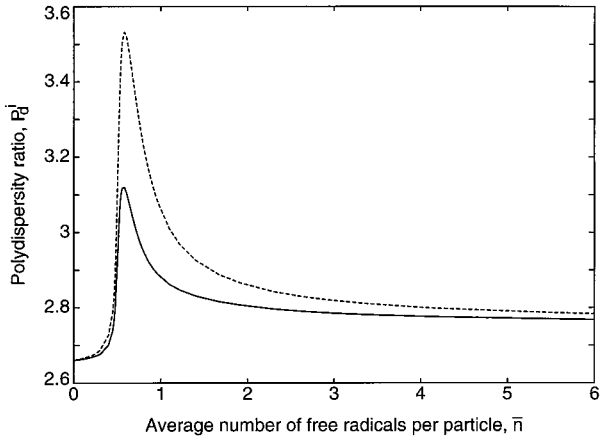

Figure 5. Polydispersity ratio as a function of the average number of active chains per particle, $\bar{n}$. Parameter values as in Table 2 but with $k_{fp} = 0$. Lines: (—) detailed model and (- - -) simplified model.

The analysis carried out in this section in terms of instantaneous MWD properties shows that a model neglecting the concept of doubly distinguished particles is able to predict correct number-average molecular weights but overestimates the values of the polydispersity ratio, especially in the range $0.4 < \bar{n} < 2$, which is typical of many emulsion systems.

However, it may be questioned how significant this error on the instantaneous properties is when they are integrated over the entire process, i.e., when the cumulative properties of the polymer are calculated. Consequently, in the following section a comparison of the two models is carried out in terms of cumulative properties.

3.2. Cumulative Properties. To permit the calculation of cumulative quantites, the equations illustrated above for the MWD calculation have been coupled to a model[17] able to account for the evolution during the polymerization process of all those quantites which determine the parameters appearing in the MWD equations.

The simulation results discussed here below refer to seeded batch reactions. The numerical values of the model parameters together with the seed characteristics are summarized in Table 3.

The case of linear chains has first been considered ($k_{fp} = k_p^* = 0$). In Figure 6a the number- and weight-average chain lengths are reported in logarithmic scale as a function of conversion. The solid line refers to the detailed model and the dashed line to the simplified model. As expected, the same number-average chain length M_n is predicted by the two models over the entire conversion range, while the weight-average chain length M_w is overestimated by the simplified model (by about 10%). This is in accordance with the fact that larger instantaneous polydispersities are calculated by the simplified model. The predicted values of the average number of radicals per particle $\bar{n}$ are reported in Figure 6b as a function of conversion. They can be seen to range from 0.5 to 1.4, i.e., they lie in a region where compartmentalization is actually expected to play a significant role (see section 3.1).

When the presence of chain transfer to polymer ($k_{fp} = 30$ cm^3/mol s, $k_p^* = 0$) is considered, the results shown in Figure 7 are obtained. In Figure 7a the

Table 3. Numerical Values of the Model Parameters Used for the Calculations of Cumulative Properties

symbol	value	dimension	meaning
B	0.939		Trommsdorff effect parameter[17]
C	3.875		Trommsdorff effect parameter[17]
$C^{sat}{}_{m,w}$	3.68×10^{-6}	mol $cm_{H_2O}{}^{-3}$	monomer water concentration at saturation
D	-0.494		Trommsdorff effect parameter[17]
k_e	2×10^{-13}	$cm^3\ s^{-1}$	entry rate constant
k_{fm}	9.07	$cm^3\ (mol\ s)^{-1}$	chain transfer to monomer rate constant
k_{fp}	30	$cm^3\ (mol\ s)^{-1}$	chain transfer to polymer rate constant
k_i	1.18×10^{-6}	s^{-1}	initiator decomposition rate constant
k_p	2.59×10^5	$cm^3\ (mol\ s)^{-1}$	propagation rate constant
k_p^*	3	$cm^3\ (mol\ s)^{-1}$	cross-linking rate constant
k_{tc}	5.97×10^9	$cm^3\ (mol\ s)^{-1}$	termination by combination rate constant
k_{td}	0	$cm^3\ (mol\ s)^{-1}$	termination by disproportionation rate constant
$[I]^0$	2.13×10^{-6}	mol cm^{-3}	initial molar concentration of initiator
M_n^{seed}	1.81×10^4		seed number-average chain length
N_P	1×10^{14}	$cm_{H_2O}{}^{-3}$	seed particle concentration
P_d^{seed}	2		seed polydispersity ratio
PM_m	104.2	g mol^{-1}	monomer molecular weight
V_m	113.8	cm^3	total volume of monomer
$V_{P,0}$	5×10^{-18}	cm^3	initial particle volume
V_w	1012.3	cm^3	total volume of water
η	1		initiator efficiency
ϕ^*	0.68		particle monomer volume fraction at saturation
ρ_m	0.878	g cm^{-3}	monomer density
ρ_p	1.05	g cm^{-3}	polymer density

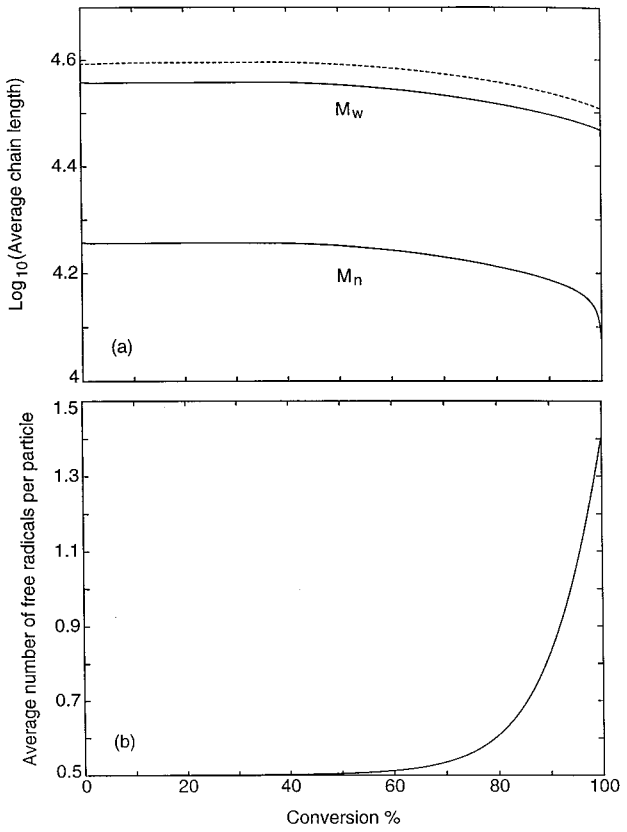

Figure 6. (a) Number- and weight-average chain length and (b) average number of active chains per particle as a function of conversion in the case of linear chains. Parameter values as in Table 3, but with $k_{fp} = k_p^* = 0$.

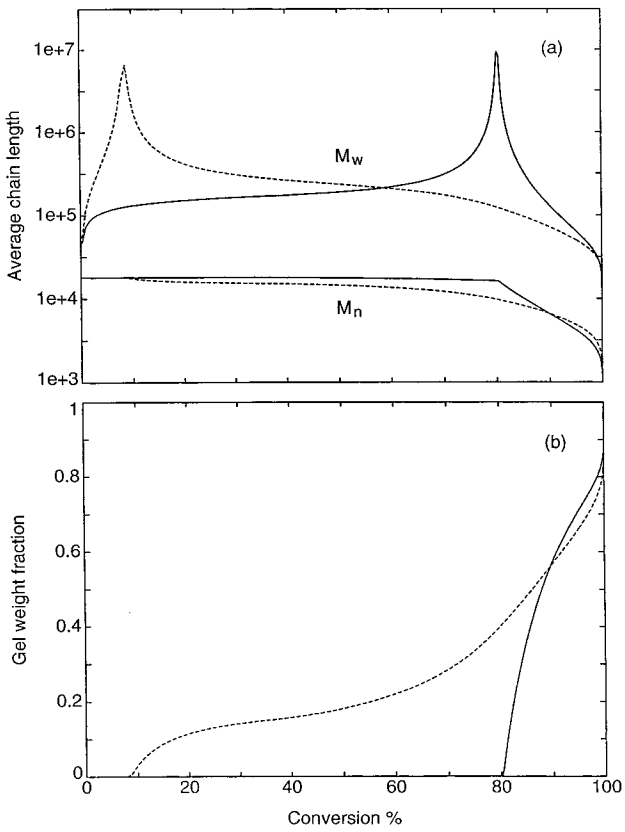

Figure 7. (a) Number- and weight-average chain length and (b) gel weight fraction as a function of conversion in the case of chain branching occurring through chain transfer to polymer. Parameter value as in Table 3, but with $k_p^* = 0$.

average chain lengths of the sol polymer fraction are plotted as a function of conversion, while in Figure 7b the gel weight fraction is reported. It can be seen that the two models yield completely different predictions in terms of weight-average chain length and of gel point. The simplified model is absolutely inadequate in this case. The marked difference between the predictions of the two models can be ascribed to the fact that the bimolecular termination mechanism is responsible for gelation in the presence of chain transfer to polymer as the sole branching mechanism. This happens because one of the requirements for the formation of gel is the presence of a mechanism connecting the chains together, and this is provided by the combination reaction in the present case. An incorrect evaluation of the way in which combination joins together the polymer chains, which is reflected by incorrect instantaneous polydispersity values calculated by the simplified model, results

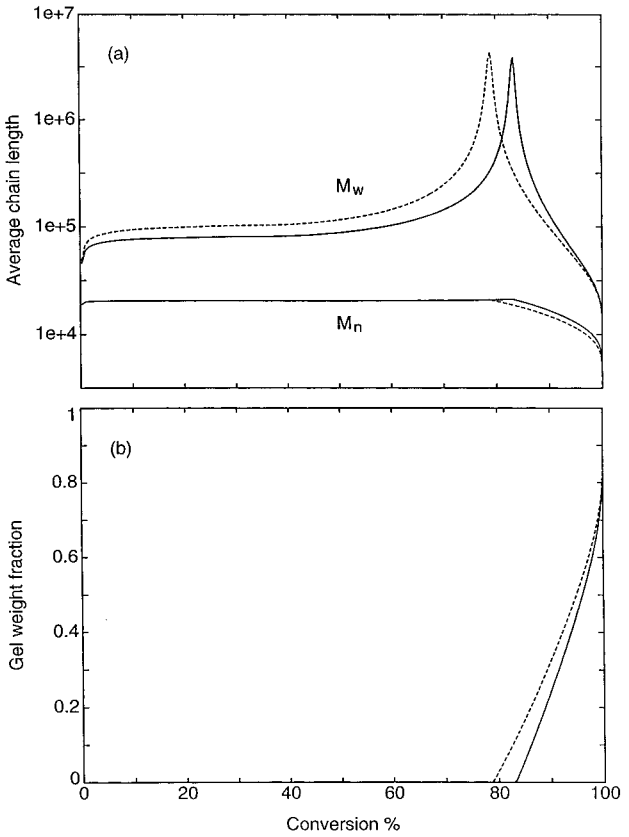

Figure 8. (a) Number- and weight-average chain length and (b) gel weight fraction as a function of conversion in the case of chain branching occurring through cross-linking. Parameter values as in Table 3, but with $k_{fp} = 0$.

in gel formation predicted to occur at much lower conversions. Considering that the $\bar{n}$ vs conversion profile coincides with that reported for linear chains in Figure 6b (all possible influences of the presence of branching on the $\bar{n}$ evolution have been neglected), it is interesting to note that the simplified model predicts gelation in a region where $\bar{n} = 0.5$, i.e., the main mode of termination is combination with very short radicals incoming from the water phase. In these conditions no gelation is obviously possible, since no coupling between branched chains can occur. With respect to this, it is to be excluded that the short incoming radicals transfer their activity to the dead polymer before the combination event, since $c \gg k_{fp}\sigma^{(1)}$ (i.e., the frequency of combination is much greater than that of chain transfer to polymer) up to over 70% conversion. The simplified model permits instead the combination of branched chains (although they belong to different particles) also in these highly compartmentalized conditions because it admits a certain amount of long−long chain coupling, as discussed in detail with regard to Figures 1 and 2. Therefore, the simplified model is shown to predict gelation in conditions where its occurrence is physically precluded.

Smaller differences between the results of the two models are found when termination by combination is no longer an essential requirement for gel formation. This can be seen in Figure 8, where the case of cross-linking as the only source of chain branching is considered ($k_p^* = 3$ cm^3/mol s, $k_{fp} = 0$). In this case the mechanism of chain coupling is provided by cross-linking itself, which alone is able to lead to the formation of a gel phase. Accordingly, the wrong evaluation of the combination mechanism through the simplified model does not induce huge inaccuracies in the evaluation of the MWD properties and of the gel point.

Finally, note that both in the case of chain transfer to polymer and of cross-linking, the same number-average chain length M_n is predicted by the two models up to the gel point (as predicted by the simplified model). After this point, the curves move apart. This happens because it is the M_n of the sol phase which is being calculated, and this is influenced by the amount of polymer belonging to the gel phase, which is different for the two models.

4. Analysis of the Assumption of Independence of the Two Lengths of a Pair of Chains

As already mentioned in section 2.2, in the calculation of the length of a dead chain from a combination reaction, the approach leading to the simplified model considers the length of the two live chains independent one of each other. In other words, given an active chain of current lifetime $\bar{t}$, the probability that another chain growing in the same particle has lifetime t_L is simply given by the number of chains of lifetime t_L divided by the overall number of chains (in particles of the same type):

$$P_i^s(t_2 = t_L | t_1 = \bar{t}) = P_i(t_2 = t_L) = \frac{N_i'(t_e - t_L, t_L)}{iN_i(t_e)} \quad (35)$$

where $P_i^s(t_2 = t_L | t_1 = \bar{t})$ represents the conditional probability (according to the simplified model) of finding a chain of lifetime t_L in a particle of state i conditioned on the fact that a chain of lifetime $\bar{t}$ is growing in the same particle, while $P_i(t_2 = t_L)$ is the probability of finding a chain of lifetime t_L irrespective of the lifetime of the other chains. Note that here we are referring to linear chains only for simplicity.

The distribution $P_i^s(t_2 = t_L | t_1 = \bar{t})$ is normalized to one, since integration of the singly distinguished particle distribution over all current lifetimes yields the overall number of active chains in particles of state i:

$$\int_0^\infty N_i'(t_e - t_L, t_L)\, dt_L = iN_i(t_e) \quad (36)$$

Note that the integration can be carried out to infinity, instead of t_e, since the times of decay of distribution N_i', corresponding to the growth times of polymer chains in the system, are usually much smaller than experimental time t_e. This also admits the approximation $N_i'(t_e - t_L, t_L) \simeq N_i'(t_e, t_L)$ in the solution of integral 36 and in the calculation of probability 35.

The correctness of eq 35, which contains the assumption of independence of the two chain lengths, can be checked by comparing probability $P_i^s(t_2 = t_L | t_1 = \bar{t})$ to that calculated by the detailed model, which will be indicated by $P_i^d(t_2 = t_L | t_1 = \bar{t})$.

This last conditional probability can be calculated through the following statistical relation:

$$P_i^d(t_1 = \bar{t}, t_2 = t_L) = P_i(t_1 = \bar{t}) \cdot P_i^d(t_2 = t_L | t_1 = \bar{t}) \quad (37)$$

which states that the probability of extracting a pair of chains from state i particles, the first of which of lifetime $\bar{t}$ and the second of lifetime t_L, is given by the probability

of finding a chain of lifetime $\bar{t}$ times the conditional probability of finding a second chain of length t_L.

The probability $P_i^d(t_1 = \bar{t}, t_2 = t_L)$ can be calculated as the number of pairs of chains of the two given lengths divided by the total number of pairs of chains in state i particles, and again divided by two since the order of extraction of the two chains of each length must be the given one. Accordingly

$$P_i^d(t_1 = \bar{t}, t_2 = t_L) = \begin{cases} \dfrac{N_i''(t_e - \bar{t}, \bar{t} - t_L, t_L)}{i(i-1)N_i(t_e)} & \text{for } t_L < \bar{t} \\ \dfrac{N_i''(t_e - t_L, t_L - \bar{t}, \bar{t})}{i(i-1)N_i(t_e)} & \text{for } t_L > \bar{t} \end{cases} \quad (38)$$

where the former or the latter relation holds according to whether the chain of lifetime $\bar{t}$ is the older or the younger of the pair, respectively.

The probability $P_i(t_1 = \bar{t})$ is instead simply calculated as the number of chains of lifetime $\bar{t}$ divided by the overall number of chains in particles of type i:

$$P_i(t_1 = \bar{t}) = \frac{N_i'(t_e - \bar{t}, \bar{t})}{iN_i(t_e)} \quad (39)$$

Substituting eqs 38 and 39 in eq 37 one obtains:

$$P_i^d(t_2 = t_L | t_1 = \bar{t}) = \begin{cases} \dfrac{N_i''(t_e - \bar{t}, \bar{t} - t_L, t_L)}{(i-1)N_i'(t_e - \bar{t}, \bar{t})} & \text{for } t_L < \bar{t} \\ \dfrac{N_i''(t_e - t_L, t_L - \bar{t}, \bar{t})}{(i-1)N_i'(t_e - \bar{t}, \bar{t})} & \text{for } t_L > \bar{t} \end{cases} \quad (40)$$

The distribution $P_i^d(t_2 = t_L | t_1 = \bar{t})$ is normalized to one, since integration over all possible lifetimes t_L of the pairs of chains, one of which of lifetime t_L and the other of lifetime $\bar{t}$, must result in the total number of chains which make pair with a chain of lifetime $\bar{t}$:

$$\int_0^{\bar{t}} N_i''(t_e - \bar{t}, \bar{t} - t_L, t_L)\, dt_L + \int_{\bar{t}}^{\infty} N_i''(t_e - t_L, t_L - \bar{t}, \bar{t})\, dt_L = (i-1)N_i'(t_e - \bar{t}, \bar{t}) \quad (41)$$

As mentioned above, comparison of probability $P_i^s(t_2 = t_L | t_1 = \bar{t})$ (which assumes independency of the active chain lengths) to probabililty $P_i^d(t_2 = t_L | t_1 = \bar{t})$, gives a good idea about when the assumption of independency is satisfied.

As an example, let us go back to the case considered in section 3.1 of linear chains in the presence of combination as the sole termination mechanism (cf. Figure 1). The conditional probabilities P_i^s and P_i^d can be compared at values of $\bar{n}$ approaching 0.5, where the difference between the simplified and the detailed model is most significant in terms of instantaneous polydispersity, and at larger $\bar{n}$ values, where this difference tends to reduce.

Figure 9 shows the quantities $t_L P_2^s$ and $t_L P_2^d$ (i.e., in state 2 particles) as a function of t_L in the case of $\bar{n} \to 0.5$, obtained assuming the frequency of entry of radicals from the water phase $\rho = 0.01\ s^{-1}$. The other parameters correspond to those used in Figure 1 (which give $c = 0.8\ s^{-1}$). A logarithmic representation on the t_L axis has been chosen due to the very different time scales of the various curves, while multiplication of the probability densities by t_L assures that the normalization of the areas beneath the curves to one is maintained. Note that this kind of representation makes the plots in Figure 9 conceptually equivalent to weight CLDs. The probability P_2^d depends upon the value of $\bar{t}$. Accordingly, various curves are reported at different $\bar{t}$ values (solid curves). On the other hand, P_2^s is independent of $\bar{t}$ and a single curve results (dashed curve).

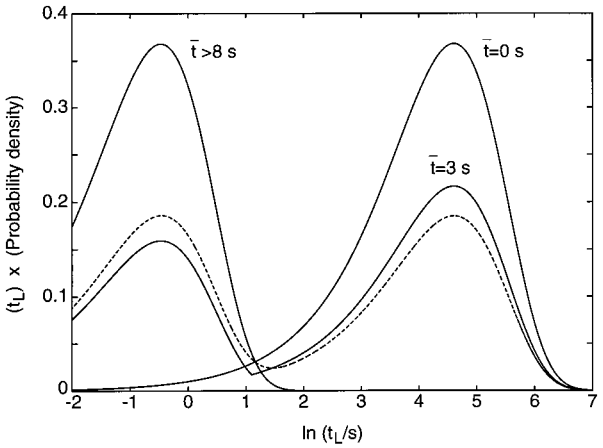

Figure 9. Probability of finding a radical of lifetime t_L in a state two particle, given another radical of lifetime $\bar{t}$ in the same particle, multipled by t_L. Bimolecular termination by combination frequency $c = 0.8\ s^{-1}$ and entry frequency $\rho = 0.01\ s^{-1}$ ($\bar{n} \to 0.5$). Lines: (—) detailed model and (- - -) simplified model.

The probabilities P_2^s and P_2^d are calculated by solving analytically systems 1 and 5 with initial conditions 3 and 9, respectively. The analytical solution is obtained from the usual eigenvalue method, i.e., given the ordinary differential system

$$\frac{d\underline{\mathbf{y}}(t)}{dt} = \underline{\underline{\mathbf{B}}}\, \underline{\mathbf{y}}(t) \quad (42)$$

(where $\underline{\underline{\mathbf{B}}}$ is independent of t) with initial conditions

$$\underline{\mathbf{y}}(t = 0) = \underline{\mathbf{y}}_0 \quad (43)$$

its analytical solution is given by

$$\underline{\mathbf{y}}(t) = \sum_j \underline{\mathbf{r}}_j\, (\underline{\mathbf{l}}_j \cdot \underline{\mathbf{y}}_0) e^{\lambda_j t} \quad (44)$$

Here, $\underline{\mathbf{r}}_j$ and $\underline{\mathbf{l}}_j$ are the right and left eigenvectors of the matrix $\underline{\underline{\mathbf{B}}}$ of system 42 corresponding to eigenvalue λ_j.

Going back to Figure 9, the strong dependence of probability P_2^d on $\bar{t}$ is shown by the marked change of the solid curves at increasing t values. An asymptotic curve is reached at high $\bar{t}$ values ($\bar{t} > 8$ in the figure). The evolution of the curves shows that a short chain has a high probability of making pair with a long one, and vice versa. Chains of intermediate lengths (e.g., $t = 3$) have instead a substantially equivalent probability of being in the presence of shorter (left hand side peak) or longer chains (right hand side peak). The dashed curve, obtained from the simplified model, would incorrectly suggest that chains of any length have the same probability of making pair either with short or with long

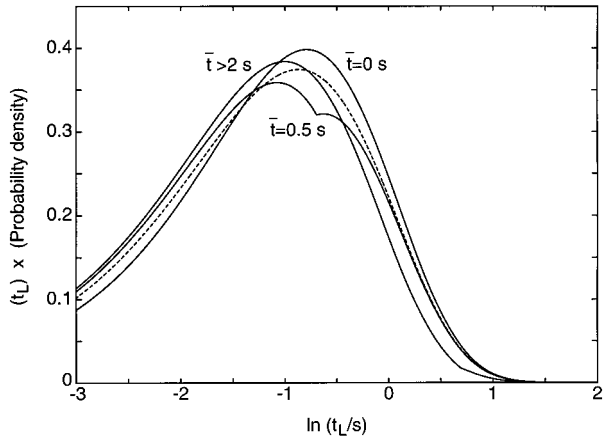

Figure 10. Probability of finding a radical of lifetime t_L in a state two particle, given another radical of lifetime $\bar{t}$ in the same particle, multiplied by t_L. Bimolecular termination by combination frequency $c = 0.8\ s^{-1}$ and entry frequency $\rho = 5\ s^{-1}$ ($\bar{n} = 2$). Lines: (—) detailed model and (- - -) simplified model.

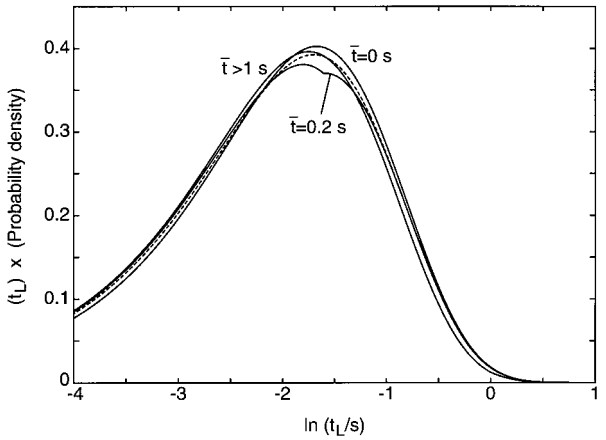

Figure 11. Probability of finding a radical of lifetime t_L in a state two particle, given another radical of lifetime $\bar{t}$ in the same particle, multiplied by t_L. Bimolecular termination by combination frequency $c = 0.8\ s^{-1}$ and entry frequency $\rho = 25\ s^{-1}$ ($\bar{n} = 4$). Lines: (—) detailed model and (- - -) simplified model.

chains. The two peaks of the dashed curve correspond to the two different contributions to the active chain distribution in state two particles, discussed with reference to Figures 1 and 2.

A similar analysis can be carried out for the probabilities P_i^s and P_i^d in state i particles with $i > 2$. Similar results are obtained, in the sense that P_i^d is significantly dependent on the value of $\bar{t}$. This indicates a strong correlation between the lengths of two chains belonging to the same particle.

The same calculations have been repeated at increasing $\bar{n}$ values. In Figure 10, $t_L P_2^s$ and $t_L P_2^d$ are reported as a function of $\ln(t_L)$ for a value of $\rho = 5\ s^{-1}$, corresponding to $\bar{n} = 2$. It can be seen that the dependence of P_2^d on $\bar{t}$ is much weaker than in the previous case and therefore the assumption of chain length independence is verified with better approximation. The probability of matching with chains of a given length is very similar at all chain lengths, and not far from that calculated by the simplified model (dashed curve). Note that the dashed curve does not present a bimodality as in the previously examined case. This shows that, at increasing values of the entry frequency ρ with respect to the combination frequency c, the distribution of the active chains is represented by a single component (differently from the case $\rho \ll c$). All that has been discussed here above for state two particles is true also for particles containing $i > 2$ radicals and is reflected in smaller errors, with respect to the case of lower $\bar{n}$ values, when the simplified model is used for the calculation of the polydispersity ratio (cf. Figure 1).

The case of a higher $\bar{n}$ value ($\bar{n} = 4$, given by $\rho = 25\ s^{-1}$), has also been examined. This yields the results presented in Figure 11, which are substantially equivalent to those shown in Figure 10, but still interesting because convergence of the P_2^d curves (solid curves) to the P_2^s curve (dashed curve) is seen to be approached, i.e., P_2^d tends to become independent of the value of $\bar{t}$ and equal to P_2^s at all t_L values. Again, this holds true also for $i > 2$. The assumption of independence of the chain lengths in a pair is thus verified better and better at increasing $\bar{n}$ values.

What is most interesting is that this independence, being related to the relative value of the entry frequency with respect to the bimolecular termination frequency, is achieved not only in particles containing a high number of radicals (which tend to be the most numerous at high $\bar{n}$ values and thus those mainly contributing to the polymer produced in the whole system) but also in particles containing few radicals, $i = 2$ in the limit. Thus, in these conditions, the properties of the produced polymer are well-calculated by use of the simplified model not only as a whole but also when focusing on the polymer produced in particles of a given state, even for low states.

5. Case Studies

Three polymerization systems, namely, styrene, methyl methacrylate, and vinyl acetate, have been studied at 50 °C. The instantaneous MWD averages have been analyzed as a function of particle radius to establish the ranges, for certain reaction conditions (temperature, initiator concentration, etc.), where the use of the simplified model is unsatisfactory. Particle radii from 5 nm up to 100 nm have been considered, i.e., from micellar size to typical dimensions of final latexes. The equations and the parameters for the systems examined have been taken from Rawlings and Ray,[18,19] with the exception of the entry constant k_{mp}, which has been assumed $k_{mp} = 6 \times 10^{19}$ cm mol^{-1} s^{-1} for all systems. The radical concentration in the water phase has been taken constant and equal to 10^{-10} mol cm^{-3}. In all cases the polymer particles have been considered monomer saturated (Smith−Ewart intervals I and II). The Trommsdorff effect has been accounted for through the empirical correlations reported by Friis and Hamielec.[20]

5.1. Styrene. Bimolecular termination has been assumed to occur by combination.[21] The dependence of the average number of radicals per particle $\bar{n}$ on particle radius r_P is shown in Figure 12a. Due to the low desorption frequencies, the system is bound for a wide range of radius values to $\bar{n} = 0.5$ (Smith−Ewart case 2, dotted line in the figure). In this range the simplified and detailed model show the greatest differences in terms of instantaneous polydispersities (Figure 12b). This could be predicted after inspection of Figure 3, where the case of a system with moderate desorption and with chain transfer to monomer was examined. In the case of styrene, an error on polydispersity of 15% up to over 20% is made by the simplified model for

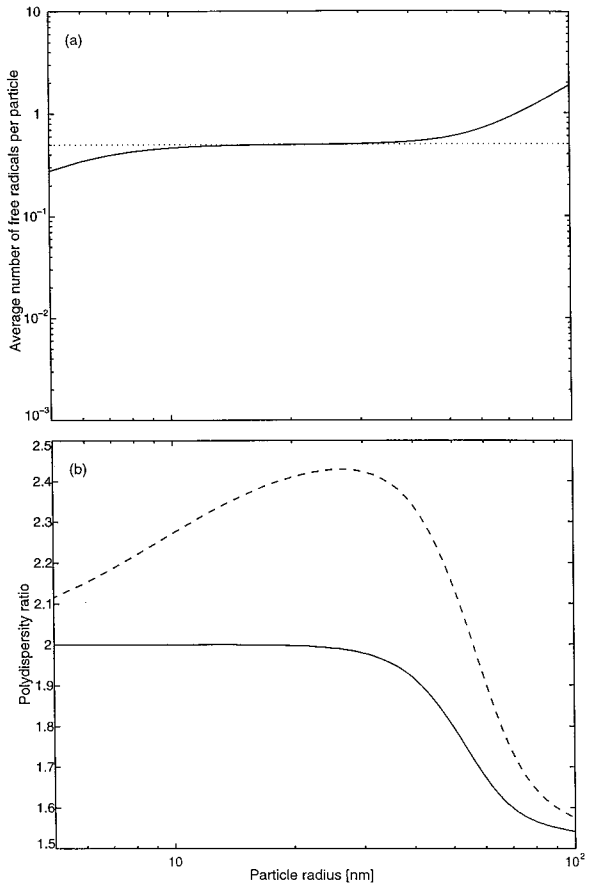

Figure 12. (a) Average number of radicals per particle (···, Smith−Ewart case 2, $\bar{n} = 0.5$) and (b) polydispersity ratio as a function of particle radius for styrene polymerization. Lines: (—) detailed model and (- - -) simplified model.

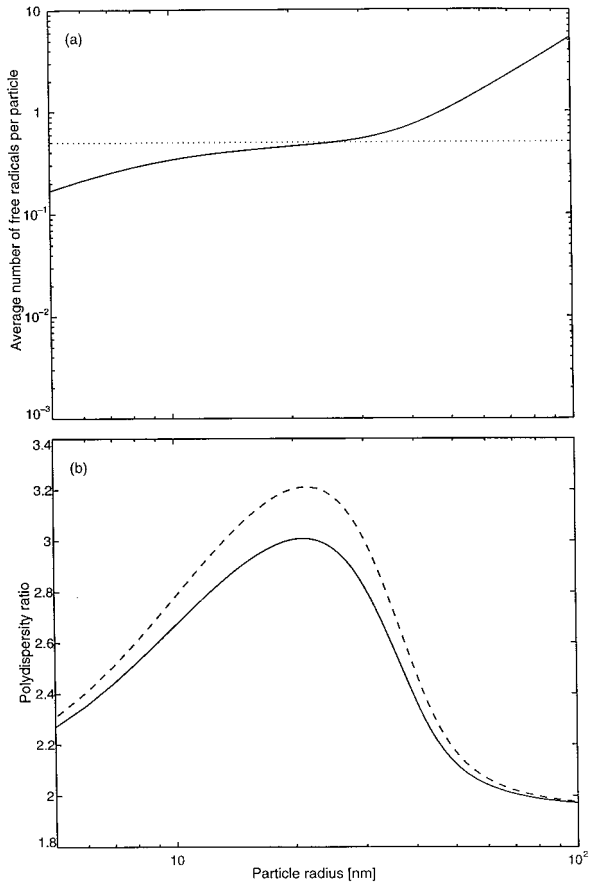

Figure 13. (a) Average number of radicals per particle (···, Smith−Ewart case 2, $\bar{n} = 0.5$) and (b) polydispersity ratio as a function of particle radius for methyl methacrylate polymerization. Lines: (—) detailed model and (- - -) simplified model.

particle radii ranging from 10 to 60 nm. At particle radii approaching 100 nm, this error tends to disappear, far before reaching "pseudo-bulk" conditions. This is in accordance with the discussion in sections 3 and 4.

5.2. Methyl Methacrylate. Bimolecular termination has been assumed to occur two-thirds by disproportionation and one-third by combination.[21] Due to higher desorption rates and a stronger Trommsdorff effect in this case, no 0.5 value plateau is observed for the average number of radicals per particle (Figure 13a). Since the amount of combination occurring in this system is limited, the error made by the simplified model in the polydispersity calculation never exceeds 7% for all particle radii (Figure 13b). Discrepancies of this magnitude would be hardly detectable by any analytical technique. The polydispersity behavior, exhibiting a maximum, is that typical of systems in which bimolecular termination by disproportionation is important.

5.3. Vinyl Acetate. The nature of the bimolecular termination mechanism for this system is still an open question.[21] The gelation technique[22] suggests that combination is the predominant termination mechanism at 25 °C. A greater amount of disproportionation may be expected at higher temperatures, for instance at the monomer boiling point where the polymerization is often performed to use the reflux condenser to remove the heat from the reaction system. Here, bimolecular termination has been assumed to occur by combination. In this way, the worst possible conditions are chosen in terms of agreement of the simplified model with the detailed one. A value of $c_p = k_{fp}/k_p = 3.96 \times 10^{-4}$ has been chosen for the chain transfer to polymer reaction.[23] The dead polymer on which this mechanism acts has been assumed to have a number-average chain length $M_n = 10^4$ and a polydispersity $P_d = 4$.

In Figure 14a, the average number of radicals per particle is reported. Very high desorption frequencies for this system keep the average number of radicals per particle far below 0.5 for low radius values. Thus, only at intermediate r_P values (e.g., 30 nm) the two models start to move significantly apart in terms of polydispersity (Figure 14b). At larger particle radii, even though chain transfer to monomer rates are very high, the discrepancy on the calculated polydispersity reaches values of 20%. Moreover, this discrepancy is a function of the polydispersity P_d of the dead polymer upon which the branching mechanism is operative. At increasing P_d values, the two models move further and further apart. Accordingly, limited differences in instantaneous polydipersities initially calculated by the two models may result crucial in cumulative terms. In section 3.2 it has been shown that accounting incorrectly for combination in a system where branching occurs through chain transfer to polymer may lead to very large errors in the weight-average molecular weight calculation. If one assumes combination as the dominant bimolecular termination, this is the case for vinyl acetate.

6. Conclusions

Through a comparison of two models having a different level of detail, it has been shown that significant

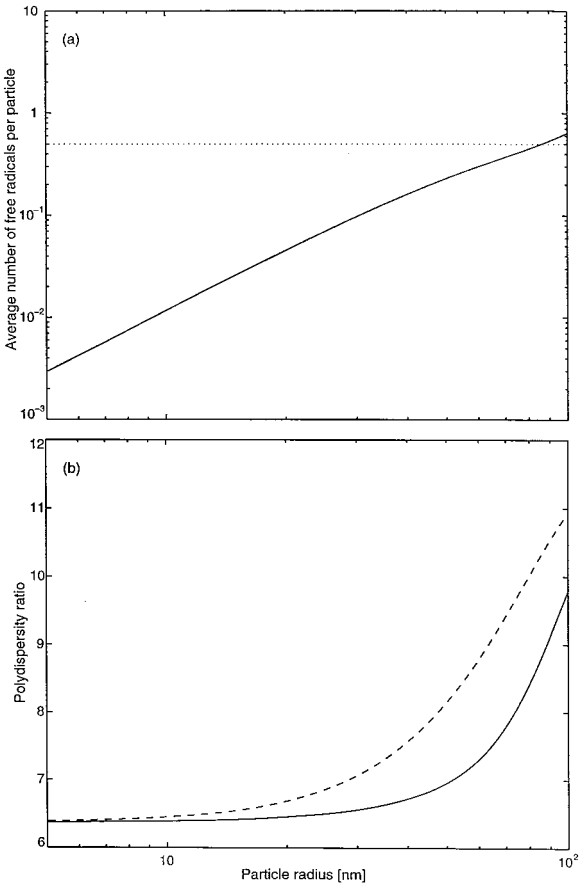

Figure 14. (a) Average number of radicals per particle (···, Smith−Ewart case 2, $\bar{n} = 0.5$) and (b) polydispersity ratio as a function of particle radius for vinyl acetate polymerization. Lines: (—) detailed model and (- - -) simplified model.

errors can be introduced in the calculation of the polydispersity ratio of a polymer produced in emulsion in the presence of termination by combination if the distribution of the lengths of the pairs of chains belonging to the same particle is not taken into consideration. This distribution is accounted for through the concept of "doubly distinguished particles" in the more detailed model.

An analysis of the instantaneous MWD properties as a function of the average number of free radicals per particle $\bar{n}$ has shown that these errors are greater in an interval of $\bar{n}$ values, typical of emulsion polymerization, ranging from 0.4 to about 2. At high $\bar{n}$ values, instead, when the entry frequency becomes much greater than the bimolecular termination frequency, the effects of compartmentalization tend to vanish and the two models give the same results. No difference is observed in the number-average chain length on the entire range of $\bar{n}$ values.

An analysis of the cumulative properties shows similar inaccuracies when neglecting the doubly distinguished particle distributions. In particular, very large errors are made when the termination by combination mechanism is responsible for gelation, such as in the case of branching occurring through chain transfer to polymer. In this case, the use of a model accounting for the compartmentalization effects in an approximate manner is absolutely unsatisfactory.

Finally, three case studies of practical importance have been analyzed to establish the ranges of polymer particle size (at least under fixed reaction conditions) where the use of the detailed model is necessary. For styrene, this is true for an intermediate range of radius values (from $r_P = 10$ nm to $r_P = 60$ nm in the conditions studied). At lower values, chain transfer to monomer is important, while at higher values the system becomes dominated by bimolecular termination. In both cases, compartmentalization effects vanish. In the case of methyl methacrylate, limited differences are found at all r_P values, due to the small combination/disproportionation ratio. For vinyl acetate, where the desorption rates are very large, significant differences arise only in the higher r_P range ($r_P > 30$ nm). The presence of a branching reaction in this case makes even limited differences in the instantaneous polydispersity values very important on a cumulative scale.

Acknowledgment. We gratefully acknowledge the financial support of the Swiss National Science Foundation (grant NF 2100-50504).

Glossary

$\underline{\underline{\mathbf{A}}}$	matrix of the coefficients for the singly distinguished particles
B_i'	distribution of the singly distinguished particles, branched
$\underline{\mathbf{B}}'$	column vector for the B_i' distribution
B_i''	distribution of the doubly distinguished particles, branched
$\underline{\mathbf{B}}''$	column vector for the B_i'' distribution
c	$= (c_c + c_d)$, overall bimolecular termination frequency
c_c	termination by combination frequency
c_d	termination by disproportionation frequency
C_m	monomer concentration in the particles
C_t	CTA concentration in the particles
$\underline{\underline{\mathbf{D}}}$	matrix of the coefficients for the doubly distinguished particles
D	CLD of the dead polymer
f	pseudo-first-order rate constant for the transfer events which do not result in desorption
G^C	distribution of the polymer terminated by combination coming from a pair of distinguishing chains, both branched, as calculated by the detailed model
$\bar{G}^C$	distribution of the polymer terminated by combination coming from a pair of distinguishing chains, both branched, as calculated by the simplified model
G^M	distribution of the polymer terminated by monomolecular mechanisms, branched
k	radical desorption frequency
k_e	rate constant for radical entry
k_{fm}	rate constant for chain transfer to monomer
k_{fp}	rate constant for chain transfer to polymer
k_{ft}	rate constant for chain transfer to CTA
k_p	rate constant for chain propagation
k_p^*	rate constant for cross-linking
k_{tc}	rate constant for termination by combination
k_{td}	rate constant for termination by disproportionation
M	monomer molecule
M_n	number-average chain length
M_n^i	instantaneous number-average chain length
M_w	weight-average chain length
n'	prelife of the older distinguishing chain
n''	prelife of the younger distinguishing chain

$\bar{n}$ average number of free radicals per particle
N maximum number of free radicals in a particle
N_A Avogadro's number
N_i distribution of the particles containing i radicals
N_i' distribution of the singly distinguished particles, linear
$\underline{\mathbf{N}}'$ column vector for the N_i' distribution
N_i'' distribution of the doubly distinguished particles, linear
$\underline{\mathbf{N}}''$ column vector for the N_i'' distribution
O_i'' distribution of the doubly distinguished particles with the older distinguishing chain branched
$\underline{\mathbf{O}}''$ column vector for the O_i'' distribution
P_d polydispersity ratio
P_d^i instantaneous polydispersity ratio
P_n dead polymer chain of length n
$[P_n]$ particle concentration of dead polymer chains of length n
$P(x_1 = \bar{x}_1)$ probability of occurrence of event $\bar{x}_1$
$P(x_1 = \bar{x}_1, x_2 = \bar{x}_2)$ probability of occurrence of event $\bar{x}_1$ followed by event $\bar{x}_2$
$P(x_2 = \bar{x}_2 | x_1 = \bar{x}_1)$ probability of occurrence of event $\bar{x}_2$ conditioned on event $\bar{x}_1$
r_P radius of a monomer swollen particle
$R_n^\bullet$ active polymer chain of length n
$R_w^\bullet$ active radical in the water phase
S^C distribution of the linear polymer terminated by combination, as calculated by the detailed model
$\bar{S}^C$ distribution of the linear polymer terminated by combination, as calculated by the simplified model
S^M distribution of the polymer terminated by monomolecular mechanisms, linear
t birth time of the (older) distinguishing chain
t' current lifetime
t'' current lifetime of the younger distinguishing chain of a pair
t_e experimental time
V^C distribution of the polymer terminated by combination coming from a pair of distinguishing chains, the older of which branched and the younger linear, as calculated by the detailed model
$\bar{V}^C$ distribution of the polymer terminated by combination coming from a pair of distinguishing chains, one of which branched and the other linear, as calculated by the simplified model
v_P volume of a monomer swollen particle
W^C distribution of the polymer terminated by combination coming from a pair of distinguishing chains, the older of which linear and the younger branched, as calculated by the detailed model
Y_i'' distribution of the doubly distinguished particles with the younger distinguishing chain branched
$\underline{Y}''$ column vector for the Y_i'' distribution

Greek Letters

α propagation frequency
γ ratio between internal double bonds and polymerized monomer units in a chain
ρ frequency of radical entry
$\sigma^{(k)}$ kth-order moment of the CLD of the dead polymer

References and Notes

(1) Katz, S.; Shinnar, R.; Saidel, G. M. *Adv. Chem. Ser.* **1969**, *91*, 145−157.
(2) Min, K. W.; Ray, W. H. *J. Macromol. Sci., Rev. Macromol. Chem.* **1974**, *C11*, 177−255.
(3) Lichti, G.; Gilbert, R. G.; Napper, D. H. *J. Polym. Sci., Polym. Chem. Ed.* **1980**, *18*, 1297−1323.
(4) Lichti, G.; Gilbert, R. G.; Napper, D. H. In *Emulsion Polymerization*; Piirma, I., Ed.; Academic: New York, 1982; p 93.
(5) Tobita, H. *Polym. React. Eng.* **1992−93**, *1*, 357−378.
(6) Charmot, D.; Guillot, J. *Polymer* **1992**, *33*, 352−360.
(7) Arzamendi, G.; Forcada, J.; Asua, J. M. *Macromolecules* **1994**, *27*, 6068−6079.
(8) Arzamendi, G.; Asua, J. M. *Macromolecules* **1995**, *28*, 7479−7490.
(9) Ghielmi, A.; Fiorentino, S.; Storti, G.; Mazzotti, M.; Morbidelli, M. *J. Polym. Sci. A: Polym. Chem.* **1997**, *35*, 827−858.
(10) Ghielmi, A.; Fiorentino, S.; Storti, G.; Morbidelli, M. *J. Polym. Sci. A: Polym. Chem.* **1998**, *36*, 1127−1156.
(11) Tobita, H.; Takada, Y.; Nomura, M. *Macromolecules* **1994**, *27*, 3804−3811.
(12) Smith, W. V.; Ewart, R. M. *J. Chem. Phys.* **1948**, *16*, 592−599.
(13) Ugelstad, J.; Hansen, F. K. *Rubber Chem. Technol.* **1976**, *49*, 536−609.
(14) Nomura, M. In *Emulsion Polymerization*; Piirma, I., Ed.; Academic: New York, 1982; p 191.
(15) Asua, J. M.; Sudol, E. D.; El-Aasser, M. S. *J. Polym. Sci. A: Polym. Chem.* **1989**, *27*, 3903−3913.
(16) Teymour, F.; Campbell, J. D. *Macromolecules* **1994**, *27*, 2460−2469.
(17) Storti, G.; Polotti, G.; Carrá, S.; Morbidelli, M. In *Polymer Reaction Engineering*; Reichert, K.-H., Moritz, H. U., Eds.; VCH: Weinheim, 1992; p 407.
(18) Rawlings, J. B.; Ray, W. H. *Polym. Eng. Sci.* **1988**, *28*, 237−256.
(19) Rawlings, J. B.; Ray, W. H. *Polym. Eng. Sci.* **1988**, *28*, 257−274.
(20) Friis, N.; Hamielec, A. E. In *Emulsion Polymerization*; Piirma, I., Gardon, J. L., Eds.; ACS Symp. Ser. 24; American Chemical Society: Washington DC, 1976; p 82.
(21) Moad, G.; Solomon, D. H. In *The chemistry of free radical polymerization*; Pergamon Press: Oxford, 1995; Chapter 5.
(22) Bamford, C. H.; Dyson, R. W.; Eastmond, G. C. *Polymer* **1969**, *10*, 885−899.
(23) Friis, N.; Goosney, D.; Wright, J. D.; Hamielec, A. E. *J. Appl. Polym. Sci.* **1974**, *18*, 1247−1259.

MA980657T